Circuit Models for Non-Faradaic CMOS Electrochemical Sensing

Philip H. Gordon*, Krishna Jayant[+], Yingqui Cao*, Kshitij Auluck*, Joshua Phelps* and Edwin C. Kan*

Email: phg35@cornell.edu

*School of Electrical and Computer Eng., Cornell University, Ithaca, NY / USA

[+]Departments of Electrical Eng. and Biological Sciences, Columbia University, New York, NY / USA

Abstract— To improve field use of ISFET devices for biological and chemical sensing, we present a parameter extraction model based on the correlation between multiple experiments in polyelectrolyte media. By correlating the quasi-static transconductance, impedance spectroscopy, transient current readout and capacitance-voltage (CV) measurements, we can decouple the physical contributions of the immobile/diffusive layer composition, overall solution resistance, surface potential drift under various electrolytic molarities, and reference electrode configurations. Hierarchical parameter extraction of the circuit components is demonstrated for mixtures of NaCl and MgCl$_2$. This method also sheds light the dynamics of double-layer competition and correlation, which is critical for biological and biochemical sensing.

Keywords—ISFET, Extended Gate, Modeling, Double-Layer, Impedance Spectroscopy, Polyelectrolyte.

I. INTRODUCTION

Ion Sensitive Field Effect Transistors (ISFET) have been in use for nearly half a century for non-Faradaic sensing of DNA , pH and biomolecules [1-4], but no unified circuit model is available for biologically realistic polyelectrolytes. Circuit network and parameters are generally extracted by one mode of sensing, but many aspects of the solid-electrolyte interface can affect readout accuracy and reliability if not properly modeled. Quasi-static transconductance sweeps give a measure of the surface potential and charge at the interface, but they are also influenced by the choice of fluidic electrodes and hysteresis from previous measurements. Impedance spectroscopy directly measures the mobile charge relaxations at various frequencies, but baseline levels can shift due to surface potential drift and changes in the double-layer capacitance or solution resistance. We create a unified circuit model that account for these coupled physical effects in all modes of operations, which can extract the surface potential, double layer capacitances and solution resistance in biologically relevant buffer concentrations and composition. The parametric dependence in the two-cation system is used as an illustration.

II. BACKGROUND

A. Sensing Device Structure

Two experimental setups were utilized in the model construction. The first is a two-electrode setup. A gold working/sensing electrode and either a gold pseudo-reference electrode (both 100x100 μm^2), or an Ag/AgCl reference electrode were utilized for CV and impedance spectroscopy (Fig. 1).

The second setup has the working/sensing electrode wire bonded to create a capacitive coupling to the floating gate of a transistor, creating an extended gate ISFET [5]. This setup is used for quasi-static transistor IV and transient drain current (I_d) experiments, with the same pseudo-reference and reference electrodes in the electrolyte. While CV and impedance spectroscopy experiments can be run from this setup as well, interplay with the transconductance gain requires additional treatment.
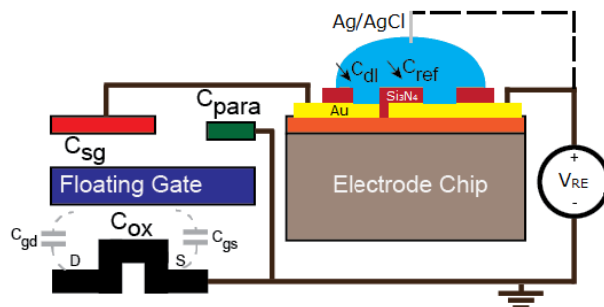

Fig 1. Device and Experimental setup. A gold electrode, silicon-nitride passivated chip is wire bonded to the sensing gate of an extended floating gate ISFET. DC bias and AC signals (V_{RE}) are provided to the solution through either an Ag/AgCl reference electrode (dotted line), or Au pseudo-reference electrode (solid line to chip).

B. Experimental Descriptions

The quasi-static transistor IV consists of sweeping the voltage of the reference electrode while monitoring I_d (with the system ground at the source). The voltage is coupled through the electrolyte, giving information on the double layer at the sensing electrode interface. Parameters of interest in this experiment are the threshold voltage of the transistor (V_{th}), which will be modulated by the net surface charge of the gate (Q_{fg}), and the subthreshold slope, which gives information on the relative electrostatics of the system.

During the transient I_d experiment, the reference electrode is set at a fixed bias I_d is recorded. ISFETs are known to have a current drift [6], and this setup monitors the stability of the surface drift. In addition, time constants of the ions in the double layer can be extracted from solution equilibration.

Impedance spectroscopy is performed by sweeping a small-signal AC voltage over a large range of frequencies, and monitoring the voltage received at the other electrode. Using a lock-in amplifier, the magnitude and phase in the spectrum is

recorded. This reveals relaxations of different components of the interface and solution, and gives small-signal component values of the double layer capacitance and global solution resistance.

A CV experiment consists of sweeping the DC bias voltage with a small AC signal on top, while monitoring the capacitance between two nodes. One can glean from a CV the flat-band potential V_{FB}, moving charge centroid, and gain insight into the makeup and dynamics of the double layer.

The electrolyte set here was a polyelectrolyte consisting of logarithmically varying concentrations of $MgCl_2$ from .3-100mM added to a base of 100mM NaCl in water (in addition to a 50mM NaCl only as control). The solution, while simple compared to biological buffers, introduces an ambiguity of the composition of the electrical double layer when composed of cations, which the integrated model can determine.

III. Modeling

Significant work has been done on modeling of each of these experimental setups individually [2, 6-8], but little work has been done correlating multiple experiments.

The IV model consists of a SPICE circuit description of the flash transistor operation, from which the surface potential and charge of the sensing electrode can be determined. The extended floating-gate ISFET setup allows for static charge Q_{fg} to be placed on the floating gate to create a threshold voltage offset such that the reference electrode need not deviate far from ground to turn on the transistor. While the solution potential should track the reference electrode even when a large bias is applied, addition of floating-gate charge reduces the possibility of hydrolysis due to the parasitic capacitance from the solution to ground (Fig. 2). Q_{fg} can also be used for molecular actuation [9], which is not further investigated here.

$$V_{fg} = \frac{Q_{fg}}{C_t} + \frac{Q_{surf}}{C_t} + \frac{C_{gs}V_{ds}}{C_t} \quad (1)$$

$$C_t = C_{ox}||C_{dep} + C_{bulk} + C_{gs} + C_{gd} + C_{sg} + C_{para} \quad (2)$$

$$I_d = k\frac{W}{L}e^{\frac{\frac{C_{ox}}{C_t}(V_{fg}-V_{th})}{V_T}} \quad (3)$$

$$I_d = k\frac{W}{L}[(V_{fg} - V_{th})V_{ds} - .5V_{ds}^2] \quad (4)$$

The Q_{fg} and Q_{surf} of (1) are the net charges on the floating gate and the sensing surface respectively. C_t is the total capacitance seen from the floating gate, consisting of the capacitances to the bulk silicon (C_{bulk}), the drain (C_{gd}), the source (C_{gs}), the sensing surface (C_{sg}), and the series combination of the oxide capacitance and channel depletion capacitance ($C_{ox}||C_{dep}$).

The model for the transistor I_d is governed by (3) and (4), where k is a semiconductor parameter pertaining to mobility of the majority carrier (electrons) and C_{ox} (120μA/V in this model). For the different transistor operating modes, (3) is used in subthreshold, while (4) is used when $V_{fg} > V_{th}$. W and L are the width (30μm) and length (1μm) of the channel in the

transistor. The voltages V_{ds}, V_{fg}, and V_T, are the drain to source voltage, floating gate voltage, and thermal voltage (26mV), respectively.

For impedance spectroscopy, the major challenge is choosing a proper circuit and fitting parameters for the system which can match the data, but remain physically meaningful. Of particular concern is the non-linearity with respect to frequency in the capacitive element and the charge transfer mechanics of the reference electrode and pseudo-reference electrode.
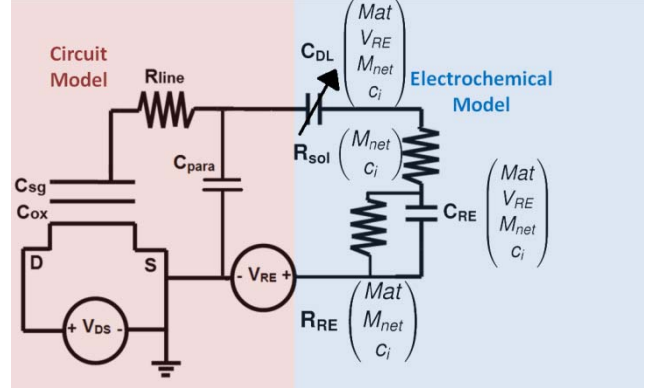

Fig 2. Circuit model for the system. Blue model is used for the CV and Impedance Spectroscopy incorporating electrochemical theory, while the red is derived for the IV experiments, and incorporates the semiconductor physics. In parentheses are the physical parameters which the circuit components depend upon: Mat (material), M_{net} (net solution molarity), c_i (concentration of each ion species), V_{RE} (reference electrode voltage). The components of the system are: R_{line} (wire and trace resistance), C_{DL} (double layer capacitance), C_{RE} (reference or pseudo-reference electrode capacitive element), R_{sol} (the electrolyte resistance), and R_{RE} (the reference electrode resistance).

$$H(s) = M_0/\left[\frac{1}{1+sR(M_{net})C(c_i,f)} * \frac{1}{1+sR(M_{net})C_0}\right] \quad (5)$$

$$C(c_i,f) = C(c_i)f^\alpha \quad (6)$$

$H(s)$ from (5) is the Laplace transform form of the two port transfer function for the impedance spectroscopy setup. The loss due to resistive division is M_0, and the solution resistance is $R(M_{net})$. The capacitors consist of a frequency and ion concentration dependent variable capacitor $C(c_i,f)$, with α as a fitting parameter for the frequency dependence of the double layer capacitance, and C_0, a static capacitance.

The CV of an electrolyte solution here is modeled as the movement of a charge centroid towards and away from the electrode surface, along with surface potential dependent changes in the concentration profile of the cations and anions. While the physical system consists of a densely packed Stern Layer and mobile diffuse layer, the charge centroid form allows for a compact model capturing most of the features of the voltage-dependent capacitance data.

$$C_{DL-cation} = k_{cation}(c_i)\frac{b(c_i)(V_{RE}-V_{fb})^2}{b_o+b(c_i)(V_{RE}-V_{fb})^2} \quad (7)$$

$$C_{DL-anion} = k_{anion}(V_{RE} - V_{fb})^2 \quad (8)$$

Two models are utilized to capture the different double layer makeups with respect to the flatband voltage V_{fb}. When $V_{RE} < V_{fb}$, the anion (Cl$^-$) is the dominant ion in the double layer, and (8) describes the capacitance with respect to voltage. On the other hand, when $V_{RE} > V_{fb}$, the cations (Mg^{+2}, Na$^+$), have the concentrations in the double layer and (7). The isothermal form sets a hard limit on the maximum capacitance of the double layer, physically corresponding to the steric hindrance of many ions in a small area. The coefficients k sets the order of the capacitance for each ion, while $b(c_i)$ and b_0 are fitting parameters for the isotherm that incorporate the different double layer makeups possible with polyelectrolyte solutions.

IV. RESULTS

A. IV

The IV is fitted from to an n-channel floating gate MOSFET, incorporating the parasitic capacitances in the system. From the threshold voltage and subthreshold slopes extracted from the data, (1) and (2), the surface charge of the sensing electrode can be determined.

The most common use for ISFETs are as a pH sensor, with the sensing modality being the shift in threshold voltage caused by H$^+$ ions adsorbing to the surface groups. This process is chemical in nature and occurs at the interface (as opposed to a distance away in the Stern or diffuse-layer portion of the double layer) causing a sharper shift in threshold voltage than charge elsewhere. [1, 10].

As the only cause of threshold voltage shift from the changing molarities would be from the surface preferentially adsorbing Na$^+$ or Mg^{+2}, little change in net surface charge is seen in this case. In addition, as even at flatband the double layer capacitance, is much larger than the sensing electrode capacitance (C_{sg}), no change in the subthreshold slope is seen (Fig. 3).
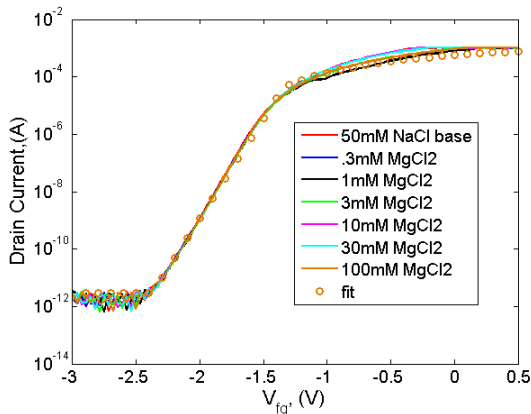

Fig 3. IV data for polyelectrolyte mix. Data are solid lines, fit is the blue circles. Small threshold shifts indicate very little surface charge change between solutions of different molarities. $V_{ds} = 1V$.

B. Impedance Spectroscopy

Utilizing a function generator to trigger and a lock-in amplifier to sample, the magnitude and phase of small signal AC excitations to the solution were collected. As per the circuit in Fig. 2, the dominant pole of the electrolyte system consists of the global solution resistance (R_{sol}) and the variable double layer capacitance (C_{dl}). For a static capacitor it would be impossible to decouple the two parameters to retrieve both from one experiment; however the frequency dependence exhibited by C_{dl} deviates from 20 dB/decade slope, which allows for the extraction C_{dl} and R_{sol} from the measurement without ambiguity.

The extraction model for the solution resistance is further improved by correlating the capacitance at 10 kHz with the CV data shown in Fig. 4. Having a known data point for a given voltage and frequency allows for more precise fitting.
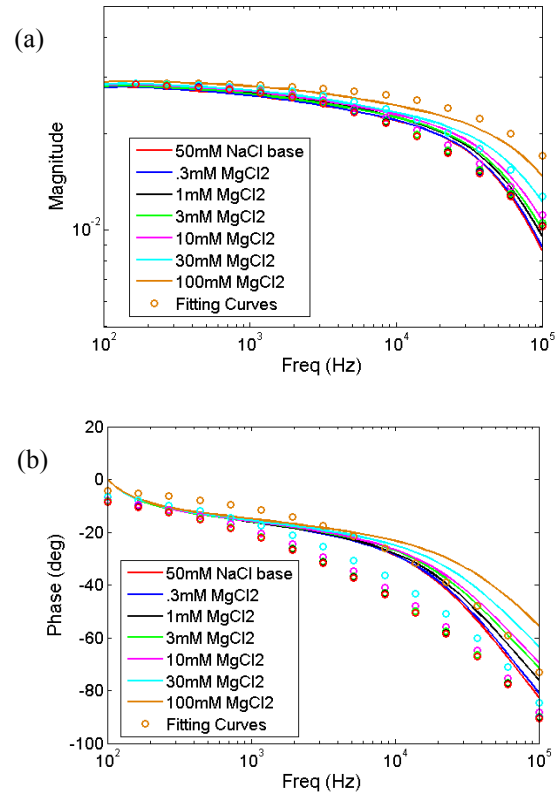

Fig. 4. Impedance spectroscopy. a) Shows the data (solid lines) and fit (circles) from the circuit model in magnitude and b) phase. While the magnitude response fit is fairly accurate, the model does not yet have a mechanism to account for the low frequency phase shift.

C. CV

The modeling of the CV data focuses around the position of the charge centroid. The work function offset between the solution and the electrodes creates a built-in potential which causes the electrical double layer. At a certain potential, known as the flatband, this offset is compensated by the applied voltage and the double layer thickness is at a maximum, corresponding to a minimum capacitance on the CV curve. At lower voltages, the double layer comprises mainly the anion

Cl⁻, while at higher voltages it contains a combination of the cations Na^+ and Mg^{+2}.

The CV data is fit to a charge centroid model integrating the cation and anion charge across the double layer. In addition, a maximum concentration of ions at the surface, (limited due to steric hindrance) is implemented, which prevents the capacitance from increasing without limit at higher voltages, as shown in Fig. 5.
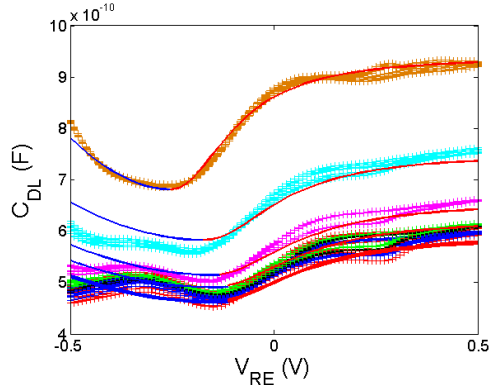

Fig. 5. CV data for Ag/AgCl reference electrode to Au sensing electrode, and fit to non-linear capacitive model. '+' signs indicate experimental data, the solid blue line indicates the Chloride ion double layer fit, while the red solid line indicates the Na^+ - Mg^{+2} competition fit. CV was swept negative to positive, then positive to negative, with hysteresis above the flatband voltage (-.25V < V_{FB} < -.1V).

D. Extraction

As per the models and equations presented, solution parameters were extracted. For brevity, only the lowest and highest solution values are shown in Table I.

TABLE I.

Parameter in 60μL H_2O	R_{sol} (Ω)	Q_{surf} @V_{th} (C/m²)	$C_{DL\text{-}avg}$ (μF/cm²)
50mM NaCl base	2040	-.0060	5.2
.3 mM $MgCl_2$	2039	-.0059	5.2
1 mM $MgCl_2$	2032	-.0059	5.3
3 mM $MgCl_2$	2011	-.0059	5.5
10 mM $MgCl_2$	1978	-.0059	5.8
30 mM $MgCl_2$	1846	-.0059	6.6
100 mM $MgCl_2$	1200	-.0058	8.3

E. Model Limitations

While the extracted capacitance, solution resistance, and surface potentials matched well with the data, there are limitations to the current model. The integrated charge sheet model fails to take into account some of the more nuanced double layer effects that can show up in more complex solutions, when ion correlation is significant. In addition, the low frequency phase effects are unaccounted for in this single non-linear capacitor model in impedance spectroscopy. The

CV model overestimates the capacitance of the anion-composed double layer, and does not have a mechanism to account for the hysteresis in the positive voltage cycle.

V. CONCLUSION

The ISFET, with its numerous operating modes is a worthwhile pursuit as a chemical and biological sensor. Despite the limitations of the present models used, the correlation between multiple measurement setups allowed for parameter extraction based primarily on polyelectrolyte data and semiconductor models which yields realistic results. This comprehensive approach will be used in future work to test detailed electrochemical models of the solution double layer. Furthermore utilizing all the available operating modes in concert with suitable models, it is possible to improve the accuracy of more complex measurements, making the device more viable for use in integrated circuits with other sampling and feedback components.

REFERENCES

[1] P. Bergveld, "Thirty years of ISFETOLOGY: What happened in the past 30 years and what may happen in the next 30 years," *Sensors and Actuators B: Chemical,* vol. 88, no. 1, pp. 1-20, 2003.

[2] M. Waleed Shinwari, M. Jamal Deen, and D. Landheer, "Study of the electrolyte-insulator-semiconductor field-effect transistor (EISFET) with applications in biosensor design," *Microelectronics Reliability,* vol. 47, no. 12, pp. 2025-2057, 2007.

[3] P. Bergveld, "Development of an Ion-Sensitive Solid-State Device for Neurophysiological Measurements," *Biomedical Engineering, IEEE Transactions on,* vol. BME-17, no. 1, pp. 70-71, 1970.

[4] K. Jayant, K. Auluck, M. Funke *et al.*, "Programmable ion-sensitive transistor interfaces. I. Electrochemical gating," *Physical Review E,* vol. 88, no. 1, pp. 012801, 2013.

[5] P. H. Gordon, K. Jayant, J. B. Phelps *et al.*, "Capacitive control of an ISFET using dielectric coated electrodes." pp. 1-4.

[6] S. Jamasb, S. Collins, and R. L. Smith, "A physical model for drift in pH ISFETs," *Sensors and Actuators B: Chemical,* vol. 49, no. 1, pp. 146-155, 1998.

[7] O. Pänke, T. Balkenhohl, J. Kafka *et al.*, "Impedance spectroscopy and biosensing," *Biosensing for the 21st Century*, pp. 195-237: Springer, 2008.

[8] M. Grattarola, G. Massobrio, and S. Martinoia, "Modeling H+-sensitive FETs with SPICE," *Electron Devices, IEEE Transactions on,* vol. 39, no. 4, pp. 813-819, 1992.

[9] K. Jayant, K. Auluck, M. Funke *et al.*, "Programmable ion-sensitive transistor interfaces. II. Biomolecular sensing and manipulation," *Physical Review E,* vol. 88, no. 1, pp. 012802, 2013.

[10] C. Jimenez-Jorquera, J. Orozco, and A. Baldi, "ISFET based microsensors for environmental monitoring," *Sensors,* vol. 10, no. 1, pp. 61-83, 2009.